

# Satellite-observed photosynthetic trends across boreal North America associated with climate and fire disturbance

Scott J. Goetz\*, Andrew G. Bunn, Gregory J. Fiske, and R. A. Houghton

Woods Hole Research Center, Woods Hole, MA 02543-0296

Communicated by George M. Woodwell, Woods Hole Research Center, Woods Hole, MA, July 20, 2005 (received for review May 5, 2005)

**We analyzed trends in a time series of photosynthetic activity across boreal North America over 22 years (1981 through 2003). Nearly 15% of the region displayed significant trends, of which just over half involved temperature-related increases in growing season length and photosynthetic intensity, mostly in tundra. In contrast, forest areas unaffected by fire during the study period declined in photosynthetic activity and showed no systematic change in growing season length. Stochastic changes across the time series were predominantly associated with a frequent and increasing fire disturbance regime. These trends have implications for the direction of feedbacks to the climate system and emphasize the importance of longer term synoptic observations of arctic and boreal biomes.**

climate change | environmental change | remote sensing | trend analysis

There has been substantial warming in the northern high latitudes in recent decades that has been associated with changes in the interannual variability of the global carbon cycle (1, 2). In the coming decades, anthropogenic climatic change will affect the productivity and physiology of plants in the northern high latitudes and further modify carbon cycling (3). Documenting and interpreting trends in plant growth at high latitudes is critical for understanding the associations and feedbacks between temperature, land cover, and atmospheric CO<sub>2</sub> (4).

The time series of normalized differenced vegetation index (NDVI) data derived from the National Oceanic and Atmospheric Administration (NOAA) Advanced Very High Resolution Radiometer (AVHRR) meteorological satellites, provides a way to continuously monitor vegetation around the globe (5). The NDVI data exploit the contrast in reflectance between the infrared and red portions of the electromagnetic spectrum and are well correlated to chlorophyll abundance and absorption of photosynthetically active radiation, which together serve as a strong proxy for gross photosynthesis (Pg) at broad spatial scales (6, 7). These data, at 8-km resolution and 15-day return interval, have been critical in developing our understanding of the trends in vegetation response to environmental conditions through the 1980s and 1990s. Earlier analyses of the satellite data indicated an increase in gross photosynthetic activity of high latitude vegetation from 1982 until 1991 (2). The eruption of Mount Pinatubo in 1991 initiated a short-term cooling of the globe (8), but photosynthetic activity continued to rise after the Pinatubo-induced cooling (9). Increased trends were primarily attributed to the earlier onset of greening and extension of growing season length (2, 8, 9). Here, we make use of an extended and refined satellite data set at high latitudes (5, 10) to show that these trends did not continue uniformly in time or space.

## Methods and Data

**Data.** We used four independent data sources across boreal North America (Canada and Alaska) to study Pg activity including: (i) a time series of satellite observations at 8-km (64

km<sup>2</sup>) spatial and 15-day temporal resolution, covering the period July 1981 to December 2003 (5, 10); (ii) a land cover typology map including agriculture, forest, and tundra categories; (iii) gridded temperature fields interpolated from ground-based meteorological stations over the period 1981 to 2000; and (iv) digital maps of wildfire extent between 1981 and 1997 (11).

The satellite NDVI data were produced as part of the National Aeronautics and Space Administration Global Inventory, Monitoring and Modeling Studies (GIMMS) project and are the most current AVHRR data on rectified Earth surface reflectance (5, 10). The GIMMS data have been calibrated to account for orbital drift, cloud cover, sensor degradation, and the emission of volcanic aerosols that attenuate the reflectance spectra. We transformed the NDVI measurements to photosynthetically active radiation absorbed by green vegetation cover, and treated this as a proxy for relative Pg ranging between 0 and 1 (6, 7). The data were stratified by vegetation type by using a map (1-km<sup>2</sup> resolution) of dominant vegetation classes produced by Natural Resources Canada (<http://geogratis.cgdi.gc.ca/clf/en>), which was resampled to match the spatial resolution of the AVHRR data. This map was used to select 10,000 random samples (64 × 10<sup>6</sup> ha) proportionally from natural vegetation cover including interior conifer forest (37.1%), deciduous forest (4.7%), mixed coniferous and deciduous forest (16.6%), and tundra (21.6%). We also used the vegetation type map to exclude a relatively small area of crop and rangeland in the Prairie Provinces of Canada. In the initial component of the analysis, any samples that had experienced fire disturbance were excluded by using the digital fire extent maps described below. Selected samples from the time series of Pg were compared with data on mean monthly temperature (°C) from Canada that had been interpolated by using thin plate spline smoothing from ground-based stations on a 10-km grid by the Canadian government's Regional, National and International Climate Modeling project ([www.glf.cfs.nrcan.gc.ca/landscape](http://www.glf.cfs.nrcan.gc.ca/landscape)). The climate data, available through January 2000, were resampled to the 8-km AVHRR data. We used data from the Canadian Fire Service Large Fire Database to identify the location of fires from 1981 to 1997, which were the most recent data available digitally (11). In a second component of the analysis, we compared the temporal trends in burned versus unburned areas during the three largest fire years (1981, 1989, and 1995). These episodic fire years also captured the early, mid, and late portions of the time series. Burned areas were screened and internally buffered to ensure adequate discrimination from unburned areas. All spatial data were coregistered to an Albers conic equal-area projection.

**Time Series Analysis.** A time series ( $y_t$ ) of seasonal Pg (the mean of June to August) was calculated for each 8-km grid cell from

Abbreviations: Pg, photosynthetic activity; NDVI, normalized differenced vegetation index; AVHRR, advanced very high resolution radiometers; ADF, augmented Dicky-Fuller.

\*To whom correspondence should be addressed at: Woods Hole Research Center, P.O. Box 269, Woods Hole, MA 02543-0296. E-mail: [sgoetz@whrc.org](mailto:sgoetz@whrc.org).

© 2005 by The National Academy of Sciences of the USA

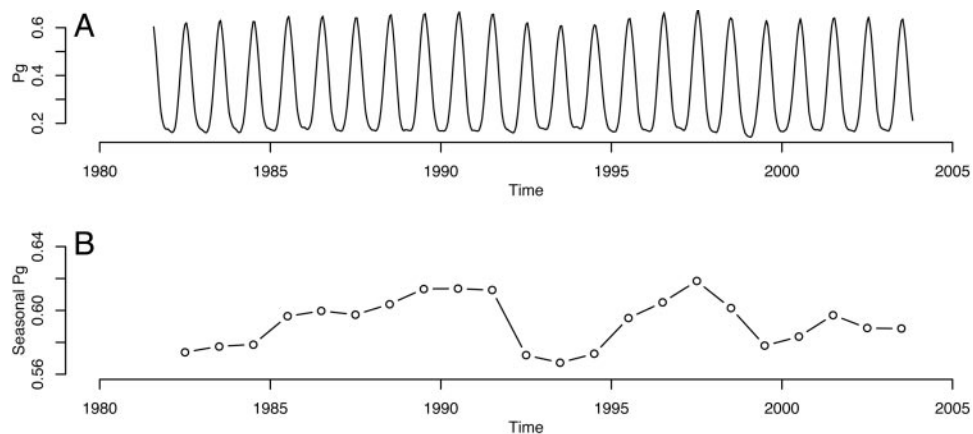


**Fig. 1.** Seasonal and growing season variations in relative Pg from 1981 to 2003 derived from the extended AVHRR record (3). The data in *A* are shown with a 3-month running mean. The data in *B* are the seasonal amplitude defined as the June, July, and August average. Data from 1981 were not included because the record is incomplete for the early part of the growing season.

1982 until 2003 (1981 was omitted because no data exist before July 1981). The time series from each grid cell in Canada and Alaska was fit by using a  $p$ th order autoregressive model

$$\Delta y_t = \alpha + \beta t + \gamma y_{t-1} + \sum_{i=1}^p \delta_i \Delta y_{t-i} + \varepsilon_t, \quad [1]$$

where  $\Delta y_t$  represents the differenced time series at a lag of  $t$  years;  $\alpha$ ,  $\beta$ ,  $\gamma$ , and  $\delta_i$  are constants;  $y_{t-1}$  is the time series at lag 1; and  $\varepsilon_t$  is random error (12). Lag orders,  $p$ , from 1 to 4 were considered, and the accepted model was that which minimized Akaike's information criterion. The residuals from the model fit were tested by using the Ljung and Box portmanteau test

$$Q = n(n+2) \sum_{i=n-1}^{n-K} \left[ \left( \frac{1}{i} \right) \sum_{k=1}^K \lambda_k^2 \right], \quad [2]$$

where  $\lambda_k$  is the autocorrelation function at lag  $k$  and  $K$  is the maximum number of lags. We used  $K = 13$  for each fitted model.  $Q < 0.05$  in all of the time series, indicating that autocorrelation was removed successfully by using the autoregressive modeling process.

**Trend Significance Tests.** Each time series was assessed for stationarity by using the augmented Dickey–Fuller (ADF) statistic  $\gamma/\text{SE}(\gamma)$  and tested for significance by using an order-adjusted 5% threshold. The series was stationary if the ADF statistic was significant (i.e., the time series returned to  $\alpha + \beta t$  after disturbance  $\varepsilon$ ). In this case, we tested for a deterministic trend by comparing  $\beta/\text{SE}(\beta)$  to the 5% critical value of the Student  $t$  distribution. The series was classified as stationary with trend if  $\beta$  was significantly different from 0; otherwise, the series was classified as stationary with no trend. The series was nonstationary if the ADF statistic was not significant. In those cases, the model was refit by ordinary least-squares regression but without the deterministic term  $\beta t$ . The test statistic in this case was as above,  $\alpha/\text{SE}(\alpha)$ . If the statistic exceeded the 5% critical value, then the series was classified as a random walk with drift; otherwise, the series was classified as a random walk with no drift. For a stationary time series with a trend, the expected change in Pg is  $\beta t$  over  $t$  years. For a series classified as a random walk with drift  $\alpha$ , the expected value of Pg at time  $t$  is  $\alpha$ .

To cross-validate the ADF test results, we also applied

Vogelsang's  $t$ - $PS_T$  stationarity test to the Pg time series (13). The Vogelsang test controls for the possibility of spurious evidence for trends due to strong serial correlation in the data. This test is valid whether the errors are stationary or have a unit root and does not require estimates of serial correlation nuisance parameters. The results of this procedure, which were largely the same as the ADF results, are presented in Table 4 and Fig. 5, which are published as supporting information on the PNAS web site.

## Results

Time series of 10,000 spatially averaged random samples (64 m ha) of natural vegetation in unburned areas reveal the seasonality of Pg at these high latitudes (Fig. 1*A*). Changes in the intensity (amplitude) of the growing season, characterized as the June through August mean, showed marked (15%) interannual variability as well as an abrupt cessation of the previously noted 1982 to 1991 trend (Fig. 1*B*). After the late-1991 Mount Pinatubo eruption, which changed the quality of incident photosynthetic radiation and cooled temperatures across much of the globe (7), mean growing season Pg again gradually increased through 1997, then declined and remained through 2003 near levels observed in the mid-1980s. Changing the window that defined the growing seasons, e.g., considering the averaged May through September

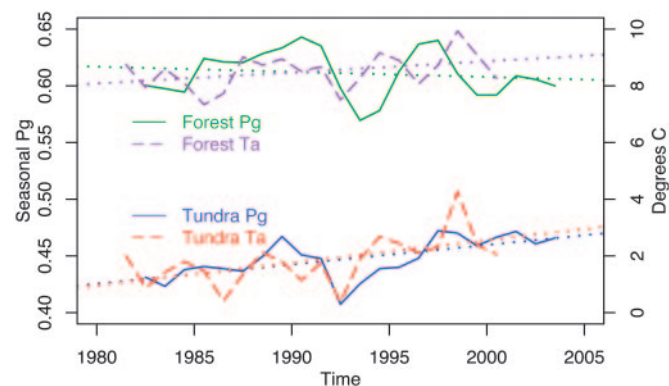


**Fig. 2.** Seasonal amplitude of relative Pg for random samples from the tundra and interior forest cover types, and independent 10-km<sup>2</sup> gridded temperature observations. Both are shown as averages for June, July, and August. The Pg data extend from 1982 to 2003 and the temperature data extend from 1982 through 2000. The dotted lines are fitted slopes and correspond to the values reported in the text.

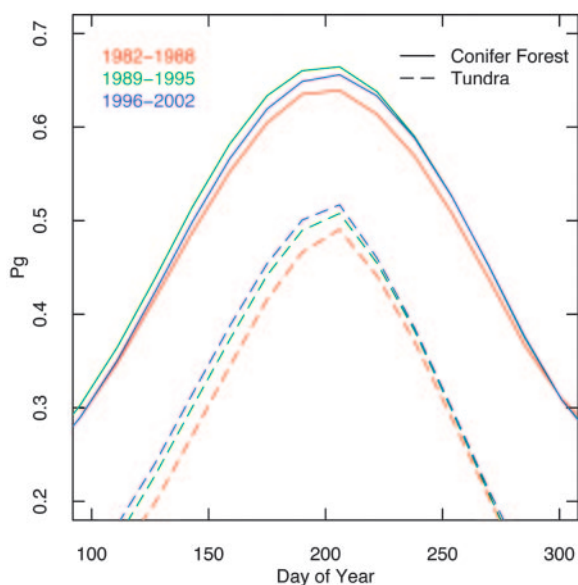


**Fig. 3.** Changes in mean phenology of relative Pg over three 6-year periods, for the same data as shown in Fig. 2. Data from 1981 were not used because the record is incomplete, and data from 2003 are not shown for these three equally partitioned time intervals: 1982–1988, 1989–1995, and 1996–2002. See text for discussion of alternate intervals.

and May through October time periods, produced essentially the same results.

The observations summarized in Fig. 1 are relevant to large-scale vegetation: climate responses and feedbacks. They indicate a substantial change in the previously noted trend in increased

photosynthesis at high latitudes for the early part of the record (2) and suggest a closer examination of the satellite record extending through the late 1990s (14, 15). Further, they capture a decline in Pg coincident with the aerosol-induced cooling brought about by the eruption of Mount Pinatubo, but also a decline in Pg during two of the warmest years in the Northern Hemisphere over the last millennium (1998 and 1999) (16), and an apparent lack of any response to the substantial warming documented across the region since (17). To examine these unexpected findings more closely, we analyzed the Pg trends not only in the context of climate, but also vegetation cover type and recent fire disturbance history.

**Vegetation Type Stratification.** When the time series of Pg was stratified by vegetation type (tundra and coniferous forest), proportioned by the relative area of each cover type on the landscape, very different responses emerged relative to temperature trends (Fig. 2). Pg in both of these dominant high latitude vegetation cover types increased between 1982 and 1990, but in years after the Pinatubo eruption, the trends diverged. Over the full 22-year series, the slope of forest areas ( $\beta$ ) was nil ( $\beta \approx 0$  [ $-4.5 \times 10^{-4}$ ],  $P = 0.521$ ,  $R^2 = 0.02$ ), whereas tundra areas continued to increase post-Pinatubo, with a slope significantly different from zero ( $\beta = 0.002$ ,  $P = 0.002$ ,  $R^2 = 0.40$ ). Mean monthly temperature, from the associated ground-based meteorological stations, increased for the areas associated with both vegetation types ( $\beta = 0.050$ ,  $P = 0.041$ ,  $R^2 = 0.19$  and  $\beta = 0.10$ ,  $P = 0.005$ ,  $R^2 = 0.38$  for conifer forest and tundra, respectively), but was a significant predictor of Pg only in tundra areas ( $P = 0.006$ ,  $R^2 = 0.39$ ) (Fig. 2).

These vegetation-specific responses to temperature trends were also reflected in the seasonality of photosynthetic activity and growing season length (Fig. 3), with tundra areas exhibiting both progressively increasing peaks and an earlier onset

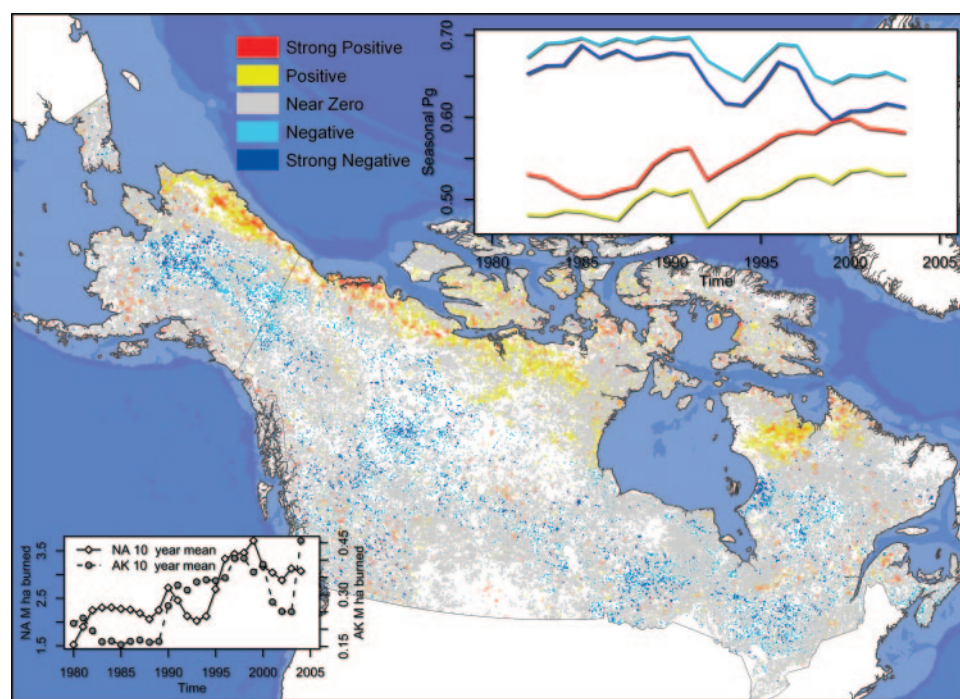


**Fig. 4.** Spatial distribution of deterministic trends in seasonal photosynthetic activity across Canada and Alaska from 1982 through 2003. The samples are colored according to the magnitude of the slope over time. Strongly negative regions are equivalent to a deterministic trend  $\beta \leq -0.005$  and cover  $38.6 \times 10^6$  ha; negative regions  $-0.005 < \beta \leq -0.0003$  ( $38.5 \times 10^6$  ha); near zero  $-0.0003 < \beta \leq 0.0003$ ; and not significantly different from zero ( $378.0 \times 10^6$  ha); positive  $0.0003 < \beta \leq 0.005$  ( $49.7 \times 10^6$  ha); and strongly positive  $\beta \geq 0.005$  ( $35.0 \times 10^6$  ha). The spatial average of mean growing season values for all areas identified as strongly negative, negative, positive, and strongly positive are shown in the upper right. Colors on the *Inset* figures correspond to those in the map. The total area burned annually across Canada and Alaska from 1980 to 2005 is shown in the bottom left (11).



**Table 1. Time series models for boreal North America (total) and the two dominant boreal vegetation cover types, tundra and forest**

	Boreal NA	Tundra	Forest
Model type	(1102 × 10 <sup>6</sup> ha)	(142 × 10 <sup>6</sup> ha)	(260 × 10 <sup>6</sup> ha)
Stationary with trend	162 (14.7%)	27.1 (19.1%)	30.9 (11.9%)
Stationary no trend	378 (34.3%)	45.1 (31.8%)	87.9 (33.9%)
Random walk with drift	349 (31.7%)	34.2 (24.1%)	100.7 (38.8%)
Random walk no drift	213 (19.3%)	35.3 (24.9%)	40.0 (15.4%)

of growth: by ≈10 days over the 22-year record. Interior forest areas, in contrast, did not reveal a consistent trend in maximum Pg or growing season length for the comparable observational periods. This finding was true whether the record was examined at regular 7-year intervals (Fig. 3), or divided into periods reflecting well defined vegetation response trends (1982–1991, 1992–1997, and 1998–2003) (see Fig. 1B).

**Spatial Distribution of Trends.** To examine the spatial distribution of the trends identified with the sampling approach, we ran the time series and trend analysis for each 64-km<sup>2</sup> grid cell location across all of Canada and Alaska and mapped the 22-year trends in growing season Pg (Fig. 4). Trends were analyzed by using the autoregressive models fitted with ordinary least-squares regression, and then classified as stationary or non-stationary. Statistical significance was determined by using both the ADF (18) and Vogelsang (13) tests. Across this 1,102 × 10<sup>6</sup> ha area, 51% of the grid cells were classified as stochastic (random) and 49% were classified as deterministic (stationary) by using the ADF tests (Table 1). Of the latter, 30% (14.7% of the total) displayed statistically significant trends, with just over half positive (52.4%) and the remainder negative (47.6%). Thus, 7.7% of the total area experienced significant increases in Pg (positive trends), and 7.0% displayed significant decreases (negative trends).

The slopes with positive trends were concentrated in tundra areas, whereas the negative slopes and stochastic drift cases were distributed throughout the interior forests (Table 2 and Fig. 4). The transition from positive to negative significant slopes occurred distinctly at the interface between forest and tundra. Further discrimination of strong positive and strong negative trends identified the location and spatial pattern of the largest changes in Pg over the time series (Fig. 4). The spatial coherence of the results with regard to land cover is striking, although we note that 62% of tundra areas and 74% of interior forest areas had slopes near zero (Table 2). Again, the results were essentially unchanged when the growing season was defined as May through September or May through October, except that a greater number of grid cells dropped

**Table 2. Magnitude of slopes for stationary models of tundra and forest vegetation cover types across boreal North America**

Slope magnitude*	Tundra, × 10 <sup>6</sup> ha	Forest, × 10 <sup>6</sup> ha
Strong negative	1.2 (1.6%)	14.4 (12.1%)
Negative	1.5 (2.1%)	11.4 (9.6%)
Near zero	45.1 (62.4%)	87.9 (74.0%)
Positive	15.9 (22.0%)	1.9 (1.6%)
Strong positive	8.6 (11.9%)	3.2 (2.7%)

\*Magnitude categories correspond to Fig. 4.

**Table 3. Area of different time series models for unburned forest and areas burned in three episodic fire years (1981, 1989, and 1995)**

Model type	Unburned, km <sup>2</sup> (%)	Burned, km <sup>2</sup> (%)
Stationary with trend	3,136 (22.4%)	576 (4.1%)
Stationary with no trend	5,440 (38.8%)	6,080 (43.4%)
Random walk with drift	3,584 (25.6%)	4,928 (35.2%)
Random walk with no drift	1,856 (13.2%)	2,432 (17.4%)

out, particularly at higher latitudes, due to an inability to fit the time series models to nonphotosynthetically active time periods.

**Burned Area Stratification.** The impact of fire disturbance on trends in Pg was assessed by using the database of large fires compiled for Canada (11), comparing burned and unburned areas of interior forest (12) for each of the four types of time series model fits (Table 1). Fire is an integral and increasingly frequent occurrence in boreal forest ecosystems (see Fig. 4 *Inset*) and varies in response to climatic warming and drying (11, 19). In the three largest fire years during the period of record (1981, 1989, and 1995), burned areas had far fewer stationary models with significant trends (4%), and a much higher percentage of stochastic behavior (Table 3). This lack of trend in burned areas is consistent with expectations, because any given area might burn at some point in the time series and then undergo a gradual recovery to pre-burn vegetation cover and density (20). A few of the negative deterministic trends in forest areas were associated with fire disturbance late in the record, mostly in interior Alaska, but burned forest areas across boreal North America were more likely to be classified as either stationary with no trend or stochastic. In contrast, areas not burned at any point in the period of record were more likely to be classified as stationary with >95% neutral or negative trends (Tables 2 and 3 and Fig. 4).

## Discussion

Growth in high latitude vegetation is widely expected to increase with rising CO<sub>2</sub> and temperature (19, 21). Our results indicate that tundra vegetation has conformed to this expectation over the past 22 years, with continued increases in photosynthetic activity as captured in the satellite data record (Fig. 4). This observation is supported by a wide and increasing range of local field measurements characterizing elevated net CO<sub>2</sub> uptake (22), greater depths of seasonal thaw (23), changes in the composition and density of herbaceous vegetation (21, 24), and increased woody encroachment in the tundra areas of North America (25).

In contrast, the response of interior forest areas to temperature change has been inconsistent with expectations of direct positive relationships between plant growth and either warming or CO<sub>2</sub> concentration. Neither the intensity nor the length of the growing season changed in a way that reflects a simple relationship with increasing temperature or CO<sub>2</sub>. In addition to the influence of fire disturbance, demonstrated here to be a key factor in detection of Pg trends, there are a number of other possible explanations for this apparent decoupling of growth and warming in forest areas, including drought stress (26, 27), nutrient limitation (28), insect and disease damage (29), and changes in resource allocation (30). Moreover, there is an emerging body of dendrochronology literature suggesting that temperature and woody growth relationships in high latitude trees are dependent on a complex interaction of landscape position and moisture availability (31, 32). We

would expect most of these processes to be manifest in the satellite observations of canopy foliage display and light harvesting (7). Nevertheless, different plant functional types, represented here by slow-growing long-lived evergreen conifers in forest areas and fast-growing short-lived deciduous herbaceous vegetation in tundra areas, should not be expected to respond similarly or uniformly to environmental change (33). Our observations indicate that the boreal biome is undergoing substantial change that varies with vegetation type,

but they raise a number of research questions concerning the response of vegetation to the interacting influences of changes in temperature, water availability, and disturbance.

T. J. Vogelsang generously supplied the computer program necessary to run the Vogelsang tests. The manuscript was improved by the constructive comments of three reviewers. We gratefully acknowledge support from the National Oceanic and Atmospheric Administration, Carbon Cycle Science Program (to S.J.G.).

- Keeling, C. D., Chin, J. F. S. & Whorf, T. P. (1996) *Nature* **382**, 146–149.
- Myneni, R. B., Keeling, C. D., Tucker, C. J., Asrar, G. & Nemani, R. R. (1997) *Nature* **386**, 698–702.
- Arctic Climate Impact Assessment (2004) *Impacts of a Warming Arctic* (Cambridge Univ. Press, Cambridge, U.K.).
- Houghton, R. A. (2003) *Glob. Change Biol.* **9**, 500–509.
- Brown, M. E., Pinzon, J. E. & Tucker, C. J. (2004) *Am. Geophys. Union EOS Trans.* **85**, 565–569.
- Myneni, R. B., Hall, F. G., Sellers, P. J. & Marshak, A. L. (1995) *IEEE Trans. Geosci. Remote Sensing* **33**, 481–486.
- Goetz, S. J. & Prince, S. D. (1999) *Adv. Ecol. Res.* **28**, 57–92.
- Lucht, W., Prentice, I. C., Myneni, R. B., Sitch, S., Friedlingstein, P., Cramer, W., Bousquet, P., Buermann, W. & Smith, B. (2002) *Science* **296**, 1687–1689.
- Slayback, D. A., Pinzon, J. E., Los, S. O. & Tucker, C. J. (2003) *Glob. Change Biol.* **9**, 1–15.
- Tucker, C. J., Pinzon, J. E., Brown, M. E., Slayback, D., Pak, E. W., Mahoney, R. E. V. & El Saleous, N., *Int. J. Remote Sensing*, in press.
- Stocks, B. J., Mason, J. A., Todd, J. B., Bosch, E. M., Wotton, B. M., Amiro, B. D., Flannigan, M. D., Hirsch, K. G., Logan, K. A., Martell, D. L. & Skinner, W. R. (December 20, 2002) *J. Geophys. Res.*, 10.1029/2001JD000484.
- Small, J., Goetz, S. J. & Hay, S. I. (2003) *Proc. Natl. Acad. Sci. USA* **100**, 15341–15345.
- Fomby, T. B. & Vogelsang, T. J. (2002) *J. Climate* **15**, 117–123.
- Nemani, R. R., Keeling, C. D., Hashimoto, H., Jolly, W. M., Piper, S. C., Tucker, C. J., Myneni, R. B. & Running, S. W. (2003) *Science* **300**, 1560–1563.
- Zhou, L. M., Tucker, C. J., Kaufmann, R. K., Slayback, D., Shabanov, N. V. & Myneni, R. B. (2001) *J. Geophys. Res.* **106**, 20069–20083.
- Mann, M. E. & Jones, P. D. (August 14, 2003) *Geophys. Res. Lett.*, 10.1029/2003GL017814.
- Jones, P. D. & Moberg, A. (2003) *J. Climate* **16**, 206–223.
- Dickey, D. A. & Fuller, W. A. (1981) *Econometrica* **49**, 1057–1072.
- Kasischke, E. S. & Stocks, B. J. (2000) *Fire, Climate Change, and Carbon Cycling in the Boreal Forest* (Springer, New York).
- Hicke, J. A., Asner, G. P., Kasischke, E. S., French, N. H. F., Randerson, J. T., Collatz, G. J., Stocks, B. J., Tucker, C. J., Los, S. O. & Field, C. B. (2003) *Glob. Change Biol.* **9**, 1145–1157.
- Chapin, F. S., McGuire, A. D., Randerson, J., Pielke, R., Baldocchi, D., Hobbie, S. E., Roulet, N., Eugster, W., Kasischke, E., Rastetter, E. B., *et al.* (2000) *Glob. Change Biol.* **6**, 211–223.
- Oechel, W. C., Vourlitis, G. L., Verfaillie, J., Crawford, T., Brooks, S., Dumas, E., Hope, A., Stow, D., Boynton, B., Nosov, V. & Zulueta, R. (2000) *Glob. Change Biol.* **6**, 160–173.
- Goulden, M. L., Wofsy, S. C., Harden, J. W., Trumbore, S. E., Crill, P. M., Gower, S. T., Fries, T., Daube, B. C., Fan, S. M., Sutton, D. J., *et al.* (1998) *Science* **279**, 214–217.
- Epstein, H. E., Calef, M. P., Walker, M. D., Chapin, F. S. & Starfield, A. M. (2004) *Glob. Change Biol.* **10**, 1325–1334.
- Sturm, M., Racine, C. & Tape, K. (2001) *Nature* **411**, 546–547.
- Barber, V. A., Juday, G. P. & Finney, B. P. (2000) *Nature* **405**, 668–673.
- Dai, A., Trenberth, K. E. & Qian, T. (2004) *J. Hydrometeorol.* **5**, 1117–1130.
- Hobbie, S. E., Nadelhoffer, K. J. & Hogberg, P. (2002) *Plant Soil* **242**, 163–170.
- Ayres, M. P. & Lombardero, M. J. (2000) *Sci. Total Environ.* **262**, 263–286.
- Gower, S. T., Krankina, O., Olson, R. J., Apps, M., Linder, S. & Wang, C. (2001) *Ecol. Appl.* **11**, 1395–1411.
- D'Arrigo, R. D., Kaufmann, R. K., D'Arrigo, R. D., Kaufmann, R. K., Davi, N., Jacoby, G. C., Laskowski, C., Myneni, R. B. & Cherubini, P. (September 24, 2004) *Glob. Biogeochem. Cycles*, 10.1029/2004GB002249.
- Wilmking, M., Juday, G. P., Barber, V. A. & Zald, H. S. J. (2004) *Glob. Change Biol.* **10**, 1724–1736.
- Reich, P. B. & Oleksyn, J. (2004) *Proc. Natl. Acad. Sci. USA* **101**, 11001–11006.